

RADIOLOGY THROUGH IMAGES

Magnetic resonance imaging in dementia[☆]

L. Raposo Rodríguez*, D.J. Tovar Salazar, N. Fernández García, L. Pastor Hernández, Ó. Fernández Guinea

Fundación Hospital de Jove, Gijón, Asturias, Spain



Received 1 November 2017; accepted 25 April 2018

KEYWORDS

Magnetic resonance imaging;
Atrophy;
Dementia;
Alzheimer's disease;
Progressive supranuclear palsy;
Vascular dementia;
Multiple system atrophy;
Parkinson's disease;
Frontotemporal dementia

Abstract

Objective: To describe and illustrate the key findings on structural magnetic resonance imaging (MRI) in the most common dementias of neurodegenerative origin: Alzheimer's disease, vascular dementia, dementia with Lewy bodies, variants of frontotemporal dementia, progressive supranuclear palsy, variants of multiple system atrophy, Parkinson dementia, and corticobasal degeneration.

Conclusion: Today the role of MRI is no longer limited to ruling out underlying causes of cognitive deterioration. MRI can show patterns of atrophy with a predictive value for certain dementias which, although not specific or unique to each disease, can help to confirm diagnostic suspicion or to identify certain processes. For this reason, it is important for radiologists to know the characteristic findings of the most common dementias.

© 2018 SERAM. Published by Elsevier España, S.L.U. All rights reserved.

PALABRAS CLAVE

Resonancia magnética;
Atrofia;
Demencia;
Enfermedad de Alzheimer;
Parálisis supranuclear

Resonancia magnética en las demencias

Resumen

Objetivo: describir los hallazgos de imagen clave en los estudios de RM estructural de las demencias de origen neurodegenerativo más frecuentes: enfermedad de Alzheimer, demencia vascular, demencia de cuerpos de Lewy, variantes de la demencia frontotemporal, parálisis supranuclear progresiva, variantes de la atrofia multisistémica, parkinson-demencia y degeneración corticobasal.

* Please cite this article as: Raposo Rodríguez L, Tovar Salazar DJ, Fernández García N, Pastor Hernández L, Fernández Guinea Ó. Resonancia magnética en las demencias. Radiología. 2018;60:476–484.

* Corresponding author.

E-mail address: luciaraposo81@hotmail.com (L. Raposo Rodríguez).

progresiva;
Demencia vascular;
Atrofia
multisistémica;
Enfermedad de
Parkinson;
Demencia
frontotemporal

Conclusión: El papel de la resonancia magnética hoy en día ya no está limitado a excluir causas subyacentes de deterioro cognitivo, sino que puede mostrar patrones de atrofia y otros datos con un alto valor predictivo para determinadas demencias que, aunque no son específicos ni únicos de cada patología, pueden ayudar a confirmar una sospecha diagnóstica o a identificar inicios tempranos de determinados procesos. Por ello es importante que los radiólogos conozcan los hallazgos típicos de las demencias más frecuentes.

© 2018 SERAM. Publicado por Elsevier España, S.L.U. Todos los derechos reservados.

Introduction

Dementia is a clinical syndrome characterized by an acquired and persistent decline of superior brain functions.

The typical final outcome is neuronal loss with reduced volume of cortical regions, which can be quantified on magnetic resonance imaging (MRI) through visual scales, or volumetric techniques of the same diagnostic accuracy.^{1,2}

The goal of this paper is to describe the key imaging findings on structural MRI studies of the most common dementias of neurodegenerative origin (Table 1) such as Alzheimer's disease (AD), vascular cognitive impairment, and other less common disorders with typical findings.

Alzheimer's disease

AD is a progressive neurodegenerative disease due to intraneuronal accumulation of tau protein (neurofibrillary tangles) and extracellular β -amyloid (senile plaques) that cause neuronal death and gliosis accompanied by cognitive impairment (CI) and early memory loss.³

Global brain atrophy is the distinctive structural finding of AD, and its distribution on the MRI shows the physiopathology of this condition.⁴ The degenerative process debuts at

Table 1 Dementias of degenerative origin.

Cortical dementia

Alzheimer's disease
Frontotemporal dementia

Dementia of vascular origin

Multi-infarct dementia
Lacunar dementia
Binswanger's disease
Amyloid angiopathy
Cerebral autosomal dominant arteriopathy with subcortical infarcts and leukoencephalopathy (CADASIL)

Dementia with Lewy bodies

Parkinson's disease
Progressive supranuclear palsy
Diffuse dementia with Lewy bodies

Other dementias

Huntington's disease
Amyotrophic lateral sclerosis
Multiple sclerosis

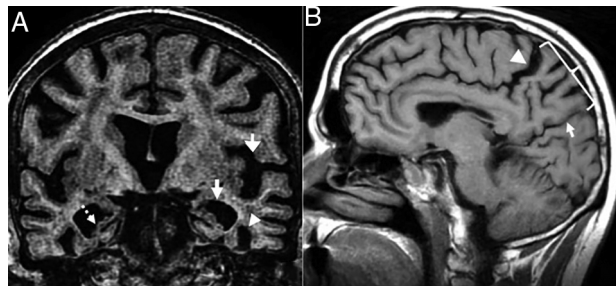


Figure 1 (A) Seventy-seven (77) year old female with Alzheimer's disease. Coronal T1 3D image. Loss of hippocampal height and volume (dotted arrow), dilation of temporal loops (closed white arrow), dilation of the parahippocampal sulcus (arrowhead), Sylvian prominence (open arrow). (B) Fifty-nine (59) year old male with cognitive impairment and suspicion of presenile Alzheimer's disease. Sagittal FLAIR T1 image. Prominence of the posterior cingulate cortex (arrowhead) due to atrophy of the *precuneus* (key) posteriorly limited by the parieto-occipital sulcus (arrow)

the medial temporal lobe (MTL), hippocampus and entorhinal cortex and spreads toward the parahippocampal space. Also, it shows early morphological and functional changes in the posterior cingulate cortex and the *precuneus*³ (Fig. 1).

Afterwards, atrophy spreads toward the temporoparietal cortex through the disconnection of the hippocampal networks due to Wallerian degeneration of white matter (WM).

In order to assess the atrophy of the MTL we can use Scheltens score – based on the choroid fissure, the temporal horn of the lateral ventricle, and hippocampal height⁵ (Table 2). The volumetric assessment is limited because it is operator dependent, but there are volumetry/segmentation and machine learning programs available in the market that are reproducible and non-operator dependent.

The serial images of the brain and hippocampal volume through MRI quantify the atrophy, the progression of the disease and its response to therapy^{5,6} and they can differentiate it from normal aging, since healthy subjects show lower rates of volume reduction than patients with AD.⁴

We should remember that global brain atrophy in the late stages of AD is not a specific finding and it can occur during the late stages of other dementias. Also, hippocampal atrophy can be seen in other conditions (hippocampal sclerosis, frontotemporal dementia, dementia with Lewy bodies [DLB], autoimmune encephalitis) and in normal aging too.⁷

Table 2 Scheltens score for measuring medial temporal lobe atrophy.

Grade 0 No atrophy
Grade 1 Only mild widening of the choroid fissure can be seen
Grade 2 Mild widening of the lateral ventricle temporal horn too (pathological in patients under 75 years old)
Grade 3 Moderate reduction of the hippocampal height too (pathological in patients over 75 years old)
Grade 4 Dramatic reduction of the hippocampal volume

Table 3 Koedam scale for measuring parietal atrophy.

Grade 0 (no cortical atrophy) The sulci of the parietal lobe and the cuneus are closed
Grade 1 (mild parietal cortical atrophy) There is a mild widening of the posterior cingulate sulcus and the parieto-occipital sulcus
Grade 2 (moderate parietal cortical atrophy) Significant widening of such sulci
Grade 3 (severe parietal atrophy) "Knife blade" atrophy. Significant widening of such sulci

Presenile or early-onset AD (under 65 years of age) usually has a family origin and is accompanied by genetic mutations of the amyloid protein metabolism.⁸ The most common finding, sometimes the only finding, is parietal atrophy with damage to the posterior cingulate cortex and the *precuneus* with a normal MTL (Fig. 1) that can be measured using the Koedam visual rating scale⁹ (Table 3).

Vascular cognitive impairment

It includes a group of dementias following hemorrhages, multiple lacunar single strategic cortical infarcts, or brain microvascular lesions.¹ Normally memory losses come late, and patients show other cognitive alterations long before developing dementia.

Small vessel vascular disease

This term refers to the rarefaction of WM visible on long-echo-time (TE) sequences as hypersignal foci due to mild stenoses of long medullary arteries. Although it also occurs with aging in asymptomatic subjects, the more WM volume damaged, the higher the risk of CI of vascular origin¹⁰ and more likely cerebrovascular risk factors will be. Arterial hypertension, tobacco, and age are the main factors that promote the progression of such lesions.¹¹

Anatomical distribution can be as important or even more important than volume. Lesions predominantly periventricular and lesions of long association pathways can produce higher CI than subcortical lesions of short association fascicles.

Table 4 Fazekas scale for measuring hyperintense lesions of cerebral white matter.

Grade 0 No lesions. Normal
Grade 1 Non-confluent focal lesions. Normal at old age.
Grade 2 Lesions initially confluent. Pathological in patients under 75 years old.
Grade 3 Confluent diffuse damage. Always pathological

Similarly, these hypersignal foci are a predictor of an early and independent risk of AD – indicative that vascular damage contributes to the development of Alzheimer's disease.¹²

Radiologically, it spares the U-shaped fibers, it can cause diffuse lesions and lacunar infarcts both in the WM and the subcortical nuclei of gray matter. The Fazekas scale is used for its evaluation and to establish the correlation among functional impairment, dementia, stroke, and death¹³ (Table 4).

We should remember that WM hyperintensities can be normal while aging.

Strategic infarcts

Are those infarcts that yet despite they are single and of a small-size can originate CI due to their capacity to functionally disconnect more extensive brain regions. They are found in the hippocampus, medial thalamus, caudate nucleus or posterior cingulate cortex¹ (Fig. 2).

Chronic microhemorrhages

We may find the following cases:

1. Arterial hypertension (basal ganglia and trunk) and hypertensive chronic encephalopathy that typically affects the basal ganglia, thalamus, encephalic trunk, cerebellum and corona radiata (Fig. 3).
2. Amyloid cerebral angiopathy. The typical findings are lobar and cortical hemorrhages in different stages and sizes, and subcortical hemorrhages at the junction of the white and gray matter. These silent hemorrhages spare the basale ganglia and associate leukoencephalopathy and atrophy.^{4,14} Magnetic susceptibility sequences are more sensitive than gradient echo sequences for the detection of such microhemorrhages, very common in AD due to their association with amyloid cerebral angiopathy, which is in turn associated with age, not with cerebrovascular risk factors. We should remember that cortical and subcortical distribution with preservation of basal ganglia, thalamus, and encephalic trunk helps us distinguish amyloid cerebral angiopathies from hypertensive hemorrhages.⁴
3. CADASIL (cerebral autosomal dominant arteriopathy with subcortical infarcts and leukoencephalopathy). It is one autosomal dominant condition due to a mutation in the NOTCH 3 gene on chromosome 19 that causes the stenosis of small-and-medium-sized caliber and long perforating

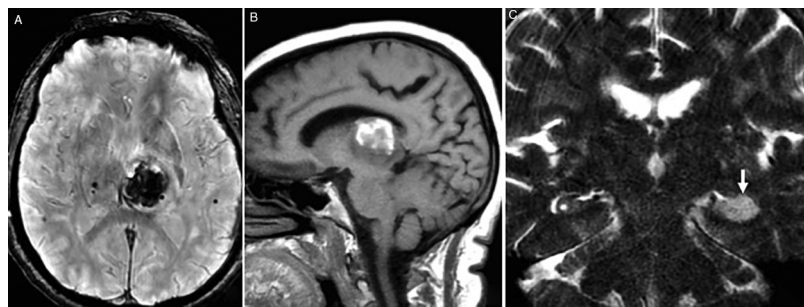


Figure 2 Examples of strategic infarcts. (A and B) Strategic hemorrhagic infarct in the left thalamus in A (axial gradient echo sequence) and B (sagittal FLAIR T1 sequence). (C) Coronal FSE-T2 image showing one hyperintense, acute ischemic lesion on the left hippocampus.

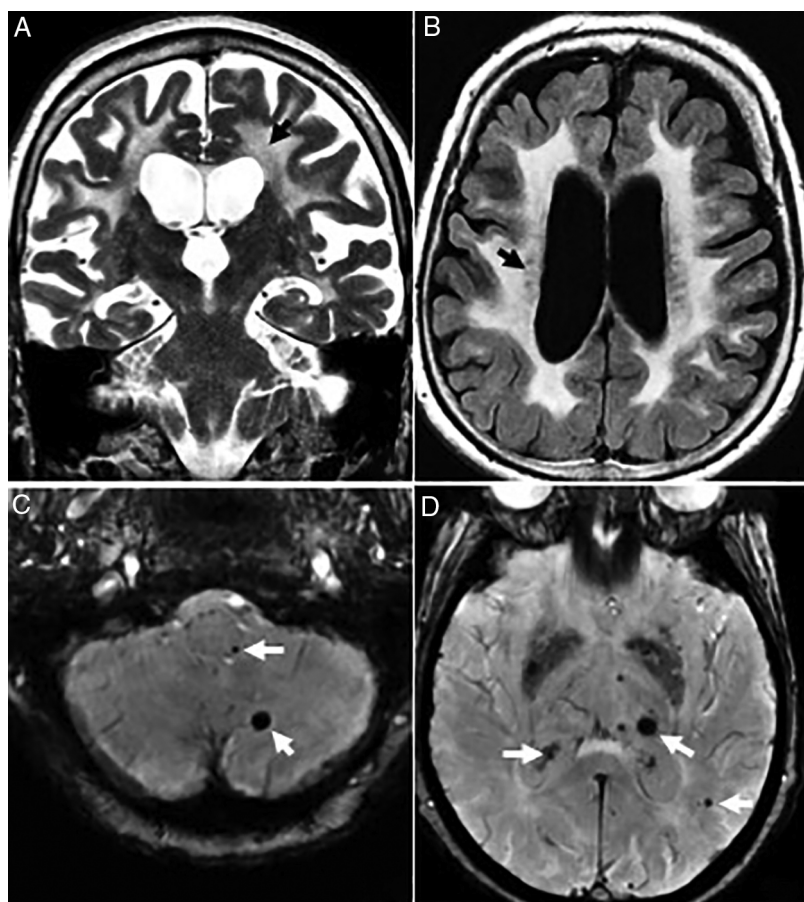


Figure 3 Seventy-seven (77) year old patient with vascular dementia. (A and B) Severe diffuse damage due to confluent hyperintense lesions of subcortical white matter and periventricular in A (coronal FSE-T2 sequence) and B (axial T2 FLAIR sequence). (C and D) Axial slices on the gradient echo sequence showing multiple microhemorrhagic foci in the cerebellum, encephalic trunk (C) and basal ganglia (D).

leptomeningeal arteries. It causes strokes, subcortical dementia, migraine with aura and mood alterations in young patients without cerebrovascular risk factors.¹⁵

The radiological findings are extensive lesions of the WM in the anterior temporal lobes and external capsules with possible infratentorial microhemorrhages, and in basal ganglia^{16,17} (Fig. 4).

Dementia with Lewy bodies

It is due to the formation of α -synuclein neurite-like aggregates to later form Lewy bodies.⁸

The presence of two (2) of the three (3) main clinical features (fluctuating CI, visual hallucinations, and Parkinsonism) is enough to give a probable diagnosis of DLB.¹⁸

Although MRIs are nonspecific individually, the voxel-based morphometry can show anterior cingulate cortex and

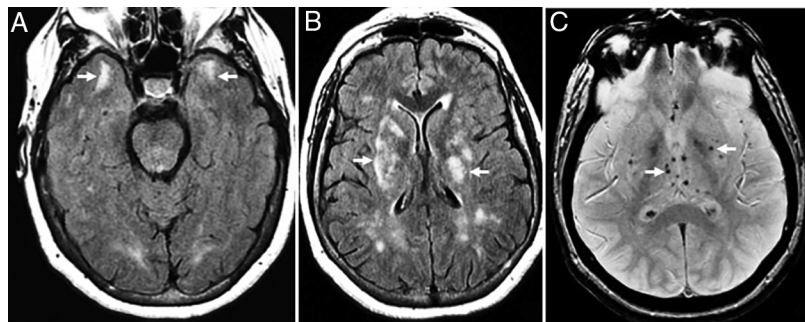


Figure 4 Thirty-eight (38) year old female with a diagnosis of CADASIL. (A) Axial T2 FLAIR image. Hyperintense lesions of subcortical white matter in typical temporal location. (B) Axial T2 FLAIR images. Multiple hyperintense lesions of diffuse distribution with a tendency toward confluence, in pathological grade, at any age. (C) Axial slices on the gradient echo sequence showing multiple microhemorrhagic foci associated with basal ganglia.

insular cortex atrophy during the prodromal stage of the disease^{19,20} and loss of temporal volume during the established stage with a distribution pattern that is different from that of AD since it spares the Ammon's horn or *subiculum*. It also damages extrahippocampal regions such as the parahippocampal gyrus that is associated with the ventral visual pathway or the striated body whose atrophy can help differentiate patients with AD from patients with DBL.

Frontotemporal dementia

It is one genetic disease that is pathologically heterogeneous and shows three (3) clinical variants: behavioral, aphasic, and semantic. The first variant is characterized by early changes of the personality and behavioral changes without initial aphasia. The aphasic stage includes progressive deficits of speech that should last, at least, two (2) years without alterations in the remaining cognitive domains (comprehension, behavior). The semantic variant is defined by fluid speech, progressive anomia and comprehension impairment accompanied by associative agnosia:^{21,22}

Behavioral. The MRI shows bilateral frontotemporal atrophy of right predominance and gliosis in the adjacent subcortical WM (Fig. 5).

Aphasic. The MRI shows an increased extra axial space in the temporolateral region due to insular and perisylvian cortex atrophy with Sylvian predominance due to atrophy of the temporal superior and inferior frontal gyri that is usually asymmetric of the left side but spares the MTL (Fig. 6).

Semantic. The most significant finding here is the basal and lateral atrophy of the temporal lobe, non-hippocampal, asymmetric and usually of left predominance with "knife blade" gyri that can be easily found on the coronal plane (Fig. 7). The presence of both hippocampal and parahippocampal atrophy is secondary. The FLAIR sequences show hypersignal of the frontotemporal subcortical WM secondary to gliosis.^{7,23}

Progressive supranuclear palsy

The progressive supranuclear palsy is considered a primary taupathy due to the accumulation of 4R tau isoforms and is

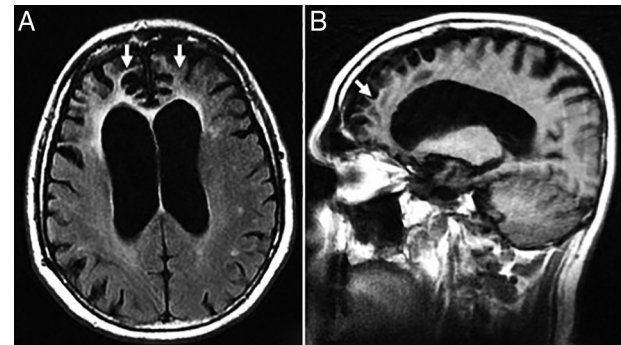


Figure 5 Seventy-two (72) year old male with frontotemporal dementia in its behavioral variant. (A) Axial FLAIR T2 sequence. Slightly asymmetric bilateral frontal atrophy of right predominance with underlying gliosis. (B) Sagittal FLAIR T1 image showing the anteroposterior gradient of atrophy.

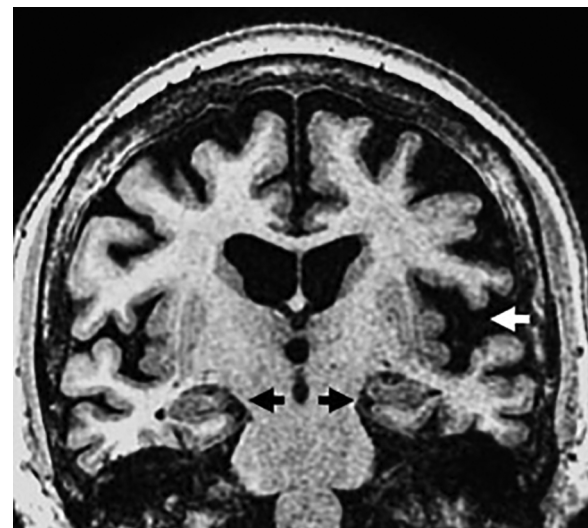


Figure 6 Seventy (70) year old patient with frontotemporal dementia in its aphasic variant. Coronal T1 3D sequence showing left asymmetric perisylvian atrophy (white arrow) with normal hippocampi and structures of the medial temporal lobe (black arrows).

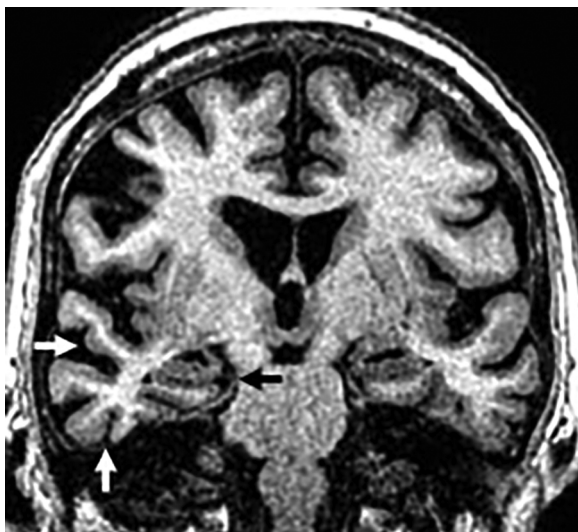


Figure 7 Cognitive impairment in a seventy-two (72) year old male with clinical manifestations of frontotemporal dementia in its semantic variant. Coronal T1 3D sequence showing basal temporal atrophy and predominant right lateral asymmetry (white arrows) with normal hippocampi (black arrow).

characterized by Parkinsonism, instability, dysarthria, dysphagia and supranuclear vertical gaze palsy.²⁴

In 75% there is midbrain atrophy with the typical hummingbird (or penguin) sign in the sagittal slices²⁵ (Fig. 8) due to a reduced correlation of the atrophied midbrain with the normal pons (the midbrain to pons area ratio <0.24). The reduced anteroposterior diameter of the midbrain at superior colliculi level from the interpeduncular fossa toward the intercollicular groove (<12 mm) translates into damage to the medial longitudinal fascicle and explains oculomotor alterations. Axial images will show the "Mickey mouse" or "morning glory" sign due to concavity of the lateral margin of the midbrain tegmentum²⁴ (Fig. 8).

The Parkinsonian index can also be used here and is obtained by multiplying the midbrain to pons area (M/P) ratio by the middle cerebellar peduncle (MCP) width-superior cerebellar peduncle (SCP) width ratio (MCP/SCP):

$$(M/P) \times (MCP/SCP) \text{ (pathological if } >13.55\text{).}$$

We should remember that midbrain atrophy is a typical yet nonspecific finding, since it can occur in healthy people above 70 years old.

These are other findings: atrophy of the anterior cingulate cortex, the superior cerebellar peduncles, the corpus callosum, dilation of the Sylvian aqueduct and the third ventricle, periaqueductal hypersignal and hypersignal of the tegmentum on T2, and putamen atrophy and hypointensity^{24,26} (Fig. 9).

Multisystemic atrophy

It is a group of neurodegenerative conditions due to intracytoplasmic inclusions of α -synuclein in oligodendroglial cells.

Although initially three (3) different entities have been described, today they are grouped into two (2) patterns accompanied by dysautonomia, being the most common of all the Parkinsonian variant (MSA-P). The typical findings are: hyperintense ring (physiological on 3T),²⁷ putamen atrophy, and globus pallidus hypointensity and atrophy (Fig. 10).

In the cerebellous variant (MSA-c) the cerebellar symptoms are predominant. The typical findings are atrophy and hypersignal of the middle cerebellar peduncles, and pontine atrophy²⁷ (Fig. 11). The degeneration of the pontine transverse fibers can show cruciform hypersignal on the axial images of the pons on the long TE sequences - something known as "hot cross bun" sign (Fig. 11). Although it is a useful marker²⁴ and initially it was thought to be pathognomonic, it can also appear in advanced stages of diseases such as vasculitis, paraneoplastic syndromes, or spinocerebellar ataxias.

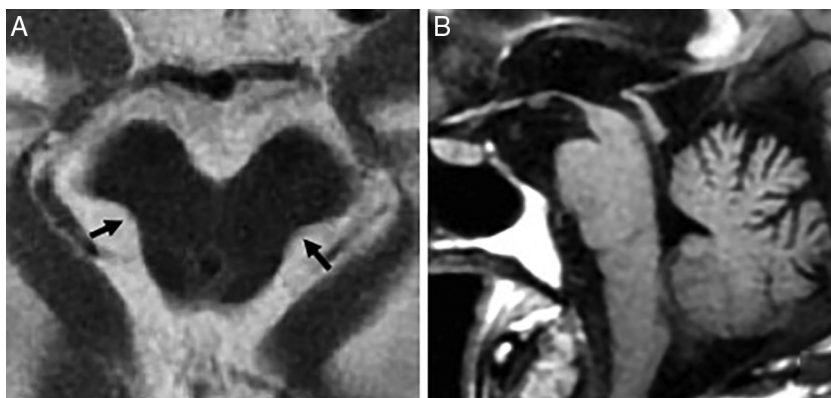


Figure 8 Progressive supranuclear palsy. (A) Axial FSE-T2 image showing midbrain atrophy. The concavity of the lateral margin of the midbrain shows the "Mickey mouse" or "morning glory" sign due to the similarity with such flower. (B) Sagittal T1 FLAIR image showing the penguin sign due to a reduced correlation between the atrophied midbrain and the normal pons on the sagittal plane. This same sequence shows the hummingbird sign due to roof atrophy (superior quadrigeminal tubercles) and the midbrain tegmentum losing its usual convex appearance and acquiring a concave morphology with relative preservation of the protuberance and the cerebellum. These structures would relate to the head (midbrain), the body (protuberance) and the hummingbird wings (cerebellum).

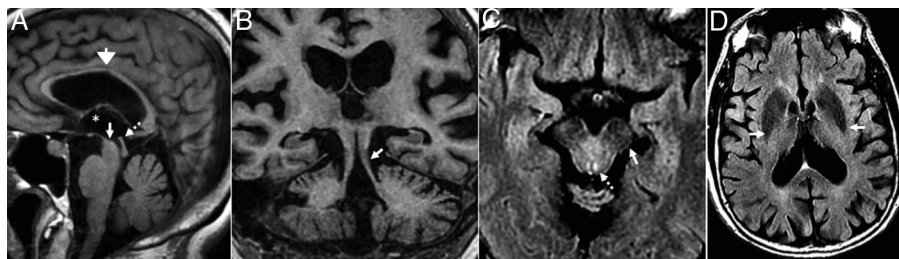


Figure 9 Progressive supranuclear palsy. (A) Sagittal T1 FLAIR image. Atrophy of the corpus callosum (open arrow), prominence of the third ventricle (asterisk), atrophy of the midbrain (arrow) and the superior colliculi (dotted arrow). (B) Coronal T1 3D image. Atrophy of the superior cerebellar peduncles. (C) Axial T2 FLAIR sequence. Periaqueductal hypersignal (dotted arrow) and effacement of the pars compacta (arrow). D) Caudate and putamen hyposignal on T2 FLAIR.

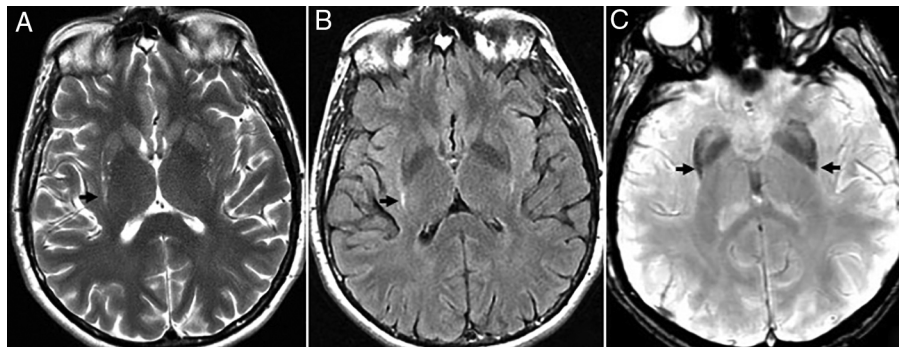


Figure 10 Multisystemic atrophy in its Parkinsonian variant. (A and B) Bilateral symmetric putamen atrophy with linear hyperintensity on T2 FSE (A) and T2 FLAIR (B) in the dorsal-lateral region of lenticular nuclei due to gliosis. (C) Axial sequence of magnetic susceptibility showing signal hypointensity in the posterior-lateral region of lenticular nucleus.

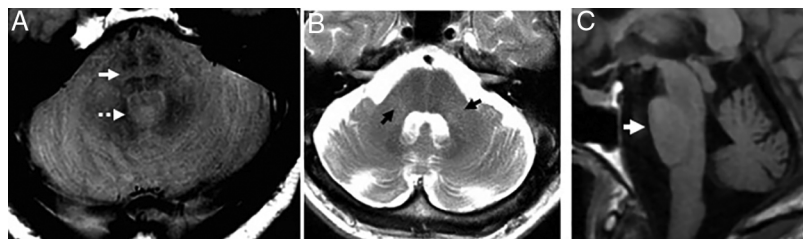


Figure 11 Multisystemic atrophy in its cerebellous variant. (A) Axial PD image showing "hot cross bun" sign (arrow) and dilation of the fourth ventricle (dotted arrow). (B) Axial FSE T2 image. Atrophy and hypersignal of the middle cerebellar peduncles (arrows) and dilation of the fourth ventricle. (C) Sagittal T1 FLAIR image. Flattened ventral region due to atrophy-induced protuberance.

Also, voxel-based morphometric studies show a more frontal and premotor distribution of atrophy in the MSA-P, and higher temporal, parietal, or lingual damage in the MSA-C.

We should remember that compared to progressive supranuclear palsy, in the MSA-C, the midbrain looks normal being the atrophic structures the pons and the cerebellum.

On many occasions there are no imaging findings to guide diagnosis.

Parkinson's disease

Between 30% and 80% of the patients with Parkinson's disease end up developing dementia. As it occurs with DLB, its origin is the intraneuronal aggregation of Lewy bodies that, in this case, damage the substantia nigra at an early stage and cause the motor symptoms of Parkinson's disease that usually precede dementia. Parkinson-dementia is typically characterized by deficits of attention and impaired

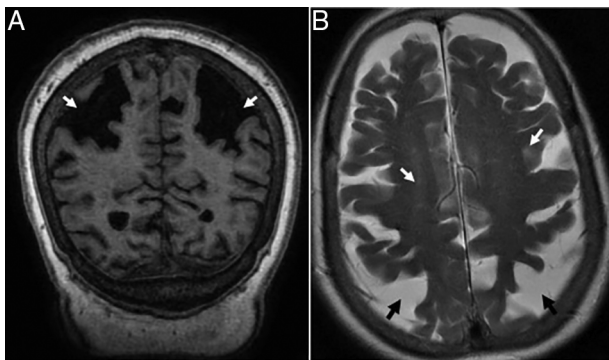


Figure 12 Corticobasal degeneration. (A) Coronal T1-weighted 3D image showing disproportionate atrophy of parietal gyri (arrows). (B) Axial T2-weighted FSE images. Hypersignal foci of the subcortical white matter (white arrows) and atrophy of parietal sulci (black arrows).

executive functions. Depression, agitation, and visual hallucinations can also be present.

The main function of the MRI is to exclude structural anomalies since, in individual analyses they look like normal findings.²⁴ However, group analyses in longitudinal studies show temporal volume losses and progression of the atrophy.²⁸

Nevertheless, there can be discreet cortical atrophy, interpeduncular cistern, substantia nigra calcifications with poor differentiation of the red nucleus, and dorsal-lateral hyposignal of putamen due to iron deposits.

The lack of "swallow sign", that is evident both in Parkinson's disease and in DLB, shows the loss of hypersignal in the nigrosome-1 of the pars compacta on magnetic susceptibility sequences.²⁹

Corticobasal degeneration

It is one heterogeneous clinicopathological entity that associates degeneration in cortical areas, basal ganglia, and substantia nigra and shows neuronal loss, gliosis, neurofibrillary tangles and plaques typically astrocytic.

Patients show atypical Parkinsonian symptoms, possible progressive apraxia with "alien hand", and some patients frontotemporal dementia.

A significant percentage of patients develop asymmetric atrophy of the parietal lobe and posterior region of the frontal lobe (Fig. 12), with possible atrophy of the ipsilateral cerebral peduncle. On the FLAIR images we may find subcortical WM hyperintensities on the atrophic frontoparietal sulci indicative of neuronal degeneration. Subthalamic hypersignal on T1 and atypical distribution of frontal subcortical gliosis in patients without a clear asymmetry in the atrophy of cerebral hemispheres have also been reported.³⁰

Basal ganglia may be damaged and atrophic.

In sum, the MRI can show patterns of atrophy and other data suggestive of certain neurodegenerative processes that radiologists should know before confirming any diagnostic suspicions.

Authors

1. Manager of the integrity of the study: LRR.
2. Study idea: LRR.
3. Study design: LRR and OFG.
4. Data mining: LRR, DJTS and NFG.
5. Data analysis and interpretation: LPH and OFG.
6. Statistical analysis: NA.
7. Reference: LRR, DJTS and NFG.
8. Writing: LRR and OFG.
9. Critical review of the manuscript with intellectually relevant remarks: LPH.
10. Approval of final version: LRR, DJTS, NFG, LPH and OFG.

Conflict of interests

The authors declare no conflict of interests associated with this article whatsoever.

References

1. Arana Fernández de Moya E. Demencias e imagen: lo básico. Radiología. 2010;52:4-17.
2. Boutet C, Chupin M, Colliot O, Sarazin M, Mutlu G, Drier A, et al. Diagnostic neuroradiology Is radiological evaluation as good as computer-based volumetry to assess hippocampal atrophy in Alzheimer's disease? Neuroradiology. 2012;54:1321-30.
3. Brown RK, Bohnen NI, Wong KK, Minoshima S, Frey KA. Brain PET in suspected dementia: patterns of altered FDG metabolism. Radiographics. 2014;34:684-701.
4. Miller-Thomas MM, Sipe AL, Benzinger TL, McConathy J, Connolly S, Schwetye KE. Multimodality review of amyloid-related diseases of the central nervous system. Radiographics. 2016;36:1147-63.
5. Sarria-Estrada S, Acevedo C, Mitjana R, Frascheri L, Siurana S, Auger C, et al. Reproducibilidad de la valoración cualitativa de la atrofia del lóbulo temporal por RM. Radiología. 2015;57:225-8.
6. Friedenberg RM. Dementia: one of the greatest fears of aging. Radiology. 2003;229:632-5.
7. Möller C, Pijnenburg YA, van der Flier WM, Versteeg A, Tijms B, de Munck JC. Alzheimer disease and behavioral variant frontotemporal dementia: automatic classification based on cortical atrophy for single-subject diagnosis. Radiology. 2016;279:838-48.
8. Jack CR. Alzheimer disease: new concepts on its neurobiology and the clinical role imaging will play. Radiology. 2012;234:64-61.
9. Koedam EL, Lehmann M, van der Flier WM, Scheltens P, Pijnenburg YA, Fox NC, et al. Visual assessment of posterior atrophy development of a MRI rating scale. Eur Radiol. 2011;21:2618-25.
10. Silbert LC, Nelson C, Howles DB, Moore MM, Kaye JA. Impact of white matter hyperintensity volume progression on rate of cognitive and motor decline. Neurology. 2008;71:108-13.
11. Gouw AA, van der Flier WM, Fazekas F, van Straaten EC, Pantoni L, Poggesi A, et al. Progression of white matter hyperintensities and incidence of new lacunes over a 3-year period. Stroke. 2008;39:1414-20.
12. Haller S, Barkhof F. Interaction of vascular damage and Alzheimer dementia: focal damage and disconnection. Radiology. 2017;282:311-3.

13. Fazekas F, Chawluk JB, Alavi A, Hurtig HI, Zimmerman RA. MR signal abnormalities at 1.5T in Alzheimer's dementia and normal aging. *AJR Am J Roentgenol.* 1987;149:351–6.
14. Guermazi A, Miaux Y, Rovira-Canellas A, Suhy J, Pauls J, López R, et al. Neuroradiological findings in vascular dementia. *Neuroradiology.* 2007;49:1–22.
15. van den Boom R, Lesnik Oberstein SA, Ferrari MD, Haan J, van Buchem MA. Cerebral autosomal dominant arteriopathy with subcortical infarcts and leukoencephalopathy: MR imaging findings at different ages-3rd-6th decades. *Radiology.* 2003;229:683–90.
16. Keyserling H, Mukundan S Jr. The role of conventional MR and CT in the work-up of dementia patients. *Neuroimag Clin N Am.* 2005;15:789–802.
17. Stojanov D, Vojinovic S, Aracki-Trenkic A, Tasic A, Benedeto-Stojanov D, Ljubisavljevic S, et al. Imaging characteristics of cerebral autosomal dominant arteriopathy with subcortical infarcts and leucoencephalopathy (CADASIL). *Bosn J Basic Med Sci.* 2015;15:1–8.
18. McKeith IG, Dickson DW, Lowe J, Emre M, O'Brien JT, Feldman H, et al. Diagnosis and management of dementia with Lewy bodies: third report of the DLB Consortium. *Neurology.* 2005;65:1863–72.
19. Blanc F, Colloby SJ, Cretin B, de Sousa PL, Demuynck C, O'Brien JT, et al. Grey matter atrophy in prodromal stage of dementia with Lewy bodies and Alzheimer's disease. *Alzheimers Res Ther.* 2016;8:31.
20. Blanc F, Colloby SJ, Philippi N, de Pétygni X, Jung B, Demuynck C, et al. Cortical thickness in dementia with Lewy bodies and Alzheimer's disease: a comparison of prodromal and dementia stages. *PLoS One.* 2015;10, e0127396. Available from: <https://doi.org/10.1371/journal.pone.0127396>
21. Lindberg O, Ostberg P, Zandbelt BB, Oberg J, Zhang Y, Andersen C, et al. Cortical morphometric subclassification of frontotemporal lobar degeneration. *AJNR Am J Neuroradiol.* 2009;30:1233–9.
22. Rohrer JD. Structural brain imaging in frontotemporal dementia. *Biochim Biophys Acta.* 2012;1822:325–32.
23. Bhogal P, Mahoney C, Graeme-Baker S, Roy A, Shah S, Fraioli F, et al. The common dementias: a pictorial review. *Eur Radiol.* 2013;23:3405–17.
24. Broski SM, Hunt CH, Johnson JB, Morreale RF, Lowe VJ, Peller PJ. Structural and functional imaging in parkinsonian syndromes. *RadioGraphics.* 2014;34:1273–92.
25. Martin-Macintosh EL, Broski SM, Johnson GB, Hunt CH, Cullen EL, Peller PJ. Multimodality imaging of neurodegenerative processes: part 2, atypical dementias. *AJR Am J Roentgenol.* 2016;207:883–95.
26. Degnan AJ, Levy LM. Neuroimaging of rapidly progressive dementias. Part 1: neurodegenerative etiologies. *AJNR Am J Neuroradiol.* 2014;35:418–23.
27. Lee WH, Lee CC, Shyu WC, Chong PN, Lin SZ. Hyperintense putaminal rim sign is not a hallmark of multiple system atrophy at 3TW. *AJNR Am J Neuroradiol.* 2005;26:2238–42.
28. Ramírez-Ruiz B, Martí MJ, Tolosa E, Bartrés-Faz D, Summerfield C, Salgado-Pineda P, et al. Longitudinal evaluation of cerebral morphological changes in Parkinson's disease with and without dementia. *J Neurol.* 2005;252:1345–52.
29. Shams S, Fällmar D, Schwarz S, Wahlund LO, van Westen D, Hansson O, et al. MRI of the swallow tail sign: a useful marker in the diagnosis of Lewy Body dementia? *AJNR Am J Neuroradiol.* 2017;38:1737–41.
30. Ukmor M, Moretti R, Torre P, Antonello RM, Longo R, Bava A. Corticobasal degeneration: structural and functional MRI and single-photon emission computed tomography. *Neuroradiol.* 2003;45:708–12.